

1974

Crack branching as predicted by the strain energy density theory /

Jing-Tang Han
Lehigh University

Follow this and additional works at: <https://preserve.lehigh.edu/etd>



Part of the [Applied Mechanics Commons](#)

Recommended Citation

Han, Jing-Tang, "Crack branching as predicted by the strain energy density theory /" (1974). *Theses and Dissertations*. 4389.
<https://preserve.lehigh.edu/etd/4389>

This Thesis is brought to you for free and open access by Lehigh Preserve. It has been accepted for inclusion in Theses and Dissertations by an authorized administrator of Lehigh Preserve. For more information, please contact preserve@lehigh.edu.

CRACK BRANCHING AS PREDICTED BY
THE STRAIN ENERGY DENSITY THEORY

by

Jing-Tang Han

A Thesis

Presented to the Graduate Committee

of Lehigh University

in Candidacy for the Degree of

Master of Science

in

Applied Mechanics

Lehigh University

1974

This thesis is accepted and approved in partial fulfillment
of the requirements for the degree of Master of Science.

May 2, 1974
(date)

George C. Sals
Professor in charge

Ferdinand P. Beer
Chairman of the
Department

ACKNOWLEDGMENTS

The author wishes to express his appreciation to Professor George C. Sih for his invaluable guidance during the preparation of this thesis. Sincere thanks are also due to Mrs. Dorothy Fielding who typed the final manuscript.

TABLE OF CONTENTS

	<u>Page</u>
ABSTRACT	1
1. INTRODUCTION	2
2. STRAIN ENERGY DENSITY FACTOR THEORY	4
3. DYNAMIC CRACK PROPAGATION	7
4. CRACK BRANCHING PHENOMENON	12
4.1 Broberg's Model	12
4.2 Yoffe's Model	15
5. DISCUSSION OF RESULTS	18
6. CONCLUSIONS AND SUGGESTIONS FOR FUTURE WORK	25
FIGURES	27
REFERENCES	39
VITA	40

LIST OF FIGURES

<u>Figure</u>	<u>Page</u>
1 Coordinates of Element	27
2 Stress Element near Crack Tip	27
3 Crack Configuration of Broberg's Model	28
4 Crack Configuration of Yoffé's Model	28
5(a) Variation of Strain Energy Density Factor for Broberg's Model ($\nu = 0.25$)	29
(b) Variation of Strain Energy Density Factor for Broberg's Model ($\nu = 0.33$)	30
6(a) Variation of Strain Energy Density Factor for Yoffé's Model ($\nu = 0.25$)	31
(b) Variation of Strain Energy Density Factor for Yoffé's Model ($\nu = 0.33$)	32
7(a) Strain Energy Density Factor versus Crack Velocity (Broberg's Model)	33
(b) Strain Energy Density Factor versus Crack Velocity (Yoffé's Model)	34
8(a) Strain Energy Density Factor in Volume Change and Shape Change versus σ_y/σ_x in Broberg's Model ($\nu = 0.25$)	35
(b) Strain Energy Density Factor in Volume Change and Shape Change versus σ_y/σ_x in Broberg's Model ($\nu = 0.33$)	36

Figure

Page

9(a) Strain Energy Density Factor in Volume Change and
Shape Change versus σ_y/σ_x in Yoffé's Model
($\nu = 0.25$)

37

(b) Strain Energy Density Factor in Volume Change and
Shape Change versus σ_y/σ_x in Yoffé's Model
($\nu = 0.33$).

38

LIST OF TABLES

<u>Table</u>		<u>Page</u>
1	Some Critical Values in Broberg's Model with $\nu = 0.25$	14
2	Some Critical Values for $\nu = 0.33$ in Broberg's Model	15
3	Some Critical Values in Yoffé's Model ($\nu = 0.25$)	16
4	Some Critical Values in Yoffé's Model ($\nu = 0.33$)	16
5	Ratios of σ_y/σ_x for Both Broberg's and Yoffé's Model	23

ABSTRACT

The strain energy density theory, which has been successfully employed in predicting crack initiation, is extended to explain the dynamic phenomenon of crack bifurcation. It is well-known that at a certain limiting velocity of crack propagation the material tends to separate in planes which are oriented at angles symmetric with reference to the original plane of material separation. This phenomenon of crack branching is predicted by the strain energy density criterion which assumes that the crack tends to follow a path along which the energy density associated with volume change is greater than that associated with shape change. The theoretical prediction of the velocity at which the crack starts to fork is too high since the effect of the crack tip radius has been neglected in the analysis.

1. INTRODUCTION

The phenomenon of crack branching is frequently observed in brittle solids such as glass, alumina, magnesia and ceramics. The problem involves in determining the direction of the branches and the magnitude of the crack velocity at which branching occurs.

Based on the criterion of maximum stress, Yoffé (1) first proposed that branching occurs when the normal stresses on two symmetrically inclined planes originating at the crack tip become greater than that on the crack plane itself. This corresponds to a crack velocity approximately equal to 0.6 of the shear wave speed. Many workers in this field have suggested to associate the smooth mirror zone of glass fracture with branching, e. g., Holloway and Johnson (2). Clark and Irwin (3) have suggested applying a critical stress intensity factor to explain branching which occurs at a certain limiting value of the crack velocity. The result can be expressed in the form $\sigma_f C_b^{1/2}$ which is assumed to be a material constant, where σ_f is the applied critical stress and C_b the length of the main crack prior to branching. Congleton and Petch (4) suggested the relationship $\sigma_f C_b^{1/2} = 2(2E r/\pi)^{1/2}$. Later, Anthony and Congleton (5) further suggested to relate stress intensity factor, K_B , at the branching to the static fracture toughness value K_C .

The present work attempts to explain crack branching by application of the strain energy density criterion which assumes that a crack will change its direction of propagation when the energy density due to volume change (dilatation) at a certain plane exceeds that due to shape change (distortion).

2. STRAIN ENERGY DENSITY FACTOR THEORY

In elastostatics the direction of crack initiation will, in general, depend on the energy state in a region ahead of the crack tip. Sih (6) has suggested to exclude from the analysis a very small region of radius r_0 surrounding the crack tip. Failure of a material element is then assumed to occur outside of this region. Such an element of incremental area $\Delta A = r \Delta \theta \Delta r$, as shown in Fig. 1 can store the following amount of strain energy per unit volume:

$$\frac{dW}{dA} = \frac{1}{r} (a_{11} k_1^2 + 2 a_{12} k_1 k_2 + a_{22} k_2^2 + a_{33} k_3^2) \quad (1)$$

Note that the higher order terms in r have been neglected; the coefficients a_{11} , a_{12} , a_{22} and a_{33} for plane strain are given by (static case),

$$a_{11} = \frac{1}{16 \mu} [(3 - 4\nu - \cos \theta)(1 + \cos \theta)] \quad (2)$$

$$a_{12} = \frac{1}{16 \mu} (2 \sin \theta) [\cos \theta - (1 - 2\nu)]$$

$$a_{22} = \frac{1}{16 \mu} [4 (1 - \nu)(1 - \cos \theta) + (1 + \cos \theta)(3 \cos \theta - 1)]$$

$$a_{33} = \frac{1}{4 \mu}$$

With ν being the Poisson's ratio and μ , the shear modulus of elasticity.

The quantity dW/dA in equation (1) is the local strain energy density function and is inversely proportional to the radial distance, r , measured from the crack tip. dW/dA becomes increasingly large as r is made to approach $r = r_0$, the boundary of the core region. The intensity of this energy field, which varies along the periphery of the circle $r = r_0$, will be denoted by S . Equation (1) may be rewritten in the following form.

$$\frac{dW}{dA} = \frac{S}{r} \quad (3)$$

in which the strain energy density factor, S , is given by

$$S = a_{11} k_1^2 + 2 a_{12} k_1 k_2 + a_{22} k_2^2 + a_{33} k_3^2 \quad (4)$$

This factor depends on θ , marking the position of the element ΔA through the coefficients a_{11} , a_{12} , a_{22} and a_{33} and therefore describes the variation of the local energy density around the region where fracture will initiate.

Sih's theory (6) contains two fundamental hypotheses on unstable crack growth as follows:

- (1) Crack initiation takes place in a direction determined by the stationary value of the strain-energy density factor, i.e.,

$$\frac{\partial S}{\partial \theta} = 0, \quad \text{at } \theta = \theta_{cr} \quad (5)$$

- (2) Crack extension occurs when the strain-energy-density factor reaches a critical value,

$$S_{cr} = S(k_1, k_2, k_3), \quad \text{for } \theta = \theta_{cr} \quad (6)$$

For dynamic case, the previous two hypotheses are developed in advance as follows:

- (1) Moving crack changes directions which are determined by $\frac{\partial S}{\partial \theta} = 0$ at $\theta = \theta_{cr}$.

- (2) Moving crack changes directions when the strain energy density factor reaches minimum of

$$S_{cr} \text{ for } \theta = \theta_{cr}.$$

The difference between S and S_{cr} is analogous to the difference between k and k_{lc} where k is a stress intensity factor and k_{lc} is known as the fracture toughness; thus S_{cr} can also be a measure of the resistance of a material to fracture.

The additional feature of the S_{cr} -theory is that the single parameter S_{cr} can simultaneously determine the fracture toughness of the material and the direction of crack initiation.

3. DYNAMIC CRACK PROPAGATION

In the opening mode of crack extension, the loads are placed symmetrically with respect to the line crack (Fig. 2) and the dynamic stress field (7) close to the tip of an advancing crack is

$$\begin{aligned}\sigma_x &= \frac{k_1}{\sqrt{2r}} F_1(S_1, S_2) [(1 + S_1^2)(2S_2^2 + 1 - S_2^2) f(S_1) \\ &\quad - 4 S_1 S_2 f(S_2)] \\ \sigma_y &= \frac{k_1}{\sqrt{2r}} F_1(S_1, S_2) [4 S_1 S_2 f(S_2) - (1 + S_2^2) f(S_1)] \\ \sigma_{xy} &= \frac{k_1}{\sqrt{2r}} 2S_1 (1 + S_2^2) F_1(S_1, S_2) [g(S_1) - g(S_2)]\end{aligned}\tag{7}$$

In equations (7), k_1 stands for the opening mode stress-intensity factor in the static theory of fracture. The parameters S_j ($j = 1, 2$) are functions of the compressional (dilatational) wave velocity C_1 and shear (equivoluminal) wave velocity C_2 in an infinitely extended region, that is

$$S_j = [1 - (C/C_j)^2]^{1/2} \quad j = 1, 2 \tag{8}$$

in which

$$C_1 = [(\lambda + 2\mu)/\rho]^{1/2}$$

$$C_2 = (\mu/\rho)^{1/2} \quad (9)$$

The crack velocity is C and λ and μ are the Lamé constants. The quantities $f(S_j)$ and $g(S_j)$ describe the angular distribution of the stresses and displacements at the loading edge of the crack. They are obtained from

$$\begin{aligned} f^2(S_j) + g^2(S_j) &= \sec \theta (1 + S_j^2 \tan^2 \theta)^{-1/2} \\ f^2(S_j) - g^2(S_j) &= \sec \theta (1 + S_j^2 \tan^2 \theta)^{-1} \end{aligned} \quad j = 1, 2 \quad (10)$$

The function $F_1(S_1, S_2)$ is the dynamic correction factor which is determined from the boundary and initial conditions of a particular problem.

The strain energy density factor for the dynamic crack problem can be obtained from the equations of elasticity. Use will be made of the strain energy function

$$W = \frac{1}{2E} [I_1^2 - 2(1 + \nu)I_2] \quad (11)$$

or

$$\begin{aligned} W = \frac{1}{2E} [&(\sigma_x + \sigma_y + \sigma_z)^2 - 2(1 + \nu)(\sigma_x \sigma_y \\ &+ \sigma_y \sigma_z + \sigma_z \sigma_x - \sigma_{xy}^2 - \sigma_{yz}^2 - \sigma_{zx}^2)] \end{aligned}$$

Where I_1 and I_2 are the first and second order invariants of the stress tensor, i.e.,

$$I_1 = \sigma_x + \sigma_y + \sigma_z \quad (12)$$

$$I_2 = \sigma_x \sigma_y + \sigma_y \sigma_z + \sigma_z \sigma_x - \sigma_{xy}^2 - \sigma_{yz}^2 - \sigma_{zx}^2$$

where ν is the Poisson ratio of the material.

For plane strain, the relation

$$\sigma_z = \nu(\sigma_x + \sigma_y) \quad (13)$$

must be observed. Substituting Equation (13) into Equation (11), and using

$$E = 2\mu (1 + \nu) \quad (14)$$

$$\lambda = \frac{2\mu\nu}{1 - 2\nu} \quad (15)$$

the strain energy density function W takes the form

$$W = \frac{1}{16\mu} [(\kappa + 1)(\sigma_x^2 + \sigma_y^2) - 2(3 - \kappa)\sigma_x\sigma_y + 8\sigma_{xy}^2] \quad (16)$$

The elastic constant K is equal to $3 - 4\nu$ for plane strain and $(3 - \nu)/(1 + \nu)$ for generalized plane stress.

From Equation (3), $dW/dA = S/r$. S represents the amplitude of the strain energy density field near the crack.

Substituting Equation (7) into Equation (16) and setting $dW/dA = S/r$ for the strain energy density per unit area, the strain energy density factor expression becomes

$$\begin{aligned}
S = \frac{k_1^2 F_1^2(s_1, s_2)}{32 \mu} \{ & (1 + s_2^2)^2 [(\kappa + 1)(2s_1^2 - s_2^2)^2 + 8(2s_1^2 \\
& + 1 - s_2^2)] f^2(s_1) \\
& + 128 s_1^2 s_2^2 f^2(s_2) \\
& - 32 s_1 s_2 (1 + s_2^2)(2s_1^2 + 2 - s_2^2) f(s_1) f(s_2) \\
& + 32 s_1^2 (1 + s_2^2) [g(s_1) - g(s_2)]^2 \}
\end{aligned}
\tag{17}$$

where

$$\begin{aligned}
f^2(s_j) &= \frac{\sec \theta}{2} [(1 + s_j^2 \tan^2 \theta)^{-1/2} + (1 + s_j^2 \tan^2 \theta)^{-1}] \\
g^2(s_j) &= \frac{\sec \theta}{2} [(1 + s_j^2 \tan^2 \theta)^{-1/2} - (1 + s_j^2 \tan^2 \theta)^{-1}]
\end{aligned}
\tag{18}$$

The strain energy density factor, S , is a complicated function of θ and C .

Because of the square power of $\tan \theta$ in $f^2(s_j)$ and $g^2(s_j)$, the strain energy density factor S is symmetric with respect to θ about the axis of $\theta = 0^\circ$.

For each pair of θ and C , two corresponding values of S can be found with opposite signs. The negative value represents the case in which a specimen is under tension while the positive value represents compression.

The $F_1(s_1, s_2)$ in Equation (17) varies from problem to problem depending on the boundary condition while the function affects

$f(S_j)$ and $g(S_j)$. ($j = 1, 2$) depend on the crack velocity and material properties.

The location of the minima of S , at θ_0 , will determine the directions of branching, with the magnitude of S reflecting the loads required for the branching to occur.

4. CRACK BRANCHING PHENOMENON

4.1 Broberg's Model

Broberg (4) considered an infinite plate with a central crack extending on both ends at a constant velocity C , as shown in Fig. 3. For this problem,

$$\begin{aligned} F_1(s_1, s_2) = & s_1 \{ [(1 + s_2^2)^2 - 4 s_1^2 s_2^2] K(s_1) \\ & - 4 s_1^2 (1 - s_2^2) K(s_2) \\ & - [4 s_1^2 + (1 + s_2^2)^2] E(s_1) + 8 s_1^2 E(s_2) \}^{-1} \end{aligned} \quad (19)$$

where K and E are complete elliptic integrals of the first and second kind, respectively.

Taking the ratio of C_1 to C_2 from equation (9)

$$C_1/C_2 = \left[\frac{\lambda + 2\mu}{\mu} \right]^{1/2}$$

and inserting equation (15) into equation (20) yields an equation of one independence for C_1/C_2 in terms of ν :

$$C_1/C_2 = \frac{2(1-\nu)}{1-2\nu}^{1/2} \quad (20)$$

Then, multiplying the crack velocity C by $1/C_2$ and $1/C_1$, respectively, i.e.,

$$C/C_2 = C/C_1 \cdot C_1/C_2 = C/C_1 \frac{2(1-\nu)}{1-2\nu}^{1/2}$$

or

$$C/C_1 = C/C_2 \frac{1-2\nu}{2(1-\nu)} \quad (21)$$

Two modified equations for S_1 and S_2 related to C/C_2 can be derived as follows:

$$S_1 = [1 - (C/C_1)^2]^{1/2} = [1 - (C/C_2)^2 \frac{1-2\nu}{2(1-\nu)}]^{1/2}$$

$$S_2 = [1 - (C/C_2)^2]^{1/2} \quad (22)$$

It is seen from the Broberg's model that S depends on C and θ in addition to the three constants K_1 , μ and ν (or κ). A normalized strain energy density factor $S^* = 32 \mu S / K_1^2$ is defined. Thus, for a given value of C/C_2 , S^* can be calculated for $-90^\circ \leq \theta \leq 90^\circ$ and various values of ν . Figure (5a) shows a plot of the normalized strain energy density factor S^* versus the angle θ for $C/C_2 = 0.5, 0.6, 0.7, 0.8$, and 0.825 with $\nu = 0.25$. It is observed that each curve has a minimum value of S at $\theta = \theta_0$. When the crack velocity increases to $C/C_2 = 0.825$, another relative minimum of the strain energy density factor appears at approximately $\theta = 55^\circ$.

Extending the theory, a separate hypothesis of Sih is needed for dynamic branching on crack growth to the dynamic case. The condition $\partial S / \partial \theta = 0$ will determine the direction of crack propagation. For crack velocities between 0° and $0.825 C_2$, $\theta_0 = 0^\circ$, the crack extends in a self similar manner. A relative minimum value of S

occurs at $\theta_o \simeq 55^\circ$ when $C = 0.825 C_2$ at which crack branching begins. $C_b = 0.825 C_2$ and $\theta_b = 55^\circ$ will be referred to as the crack branching velocity and crack branching angle.

The S_{cr} values and crack growth angles will be numerically expressed as follows:

TABLE 1

SOME CRITICAL VALUES IN BROBERG'S MODEL WITH $\nu = 0.25$

C/C_2	θ_o	$S_{cr} \cdot \frac{32 \mu}{K_1^2}$
0.5	0°	38.80
0.6	0°	12.66
0.7	0°	4.44
0.8	0°	1.91
0.825 (C_{br})	$0^\circ, 55^\circ (\theta_{cr})$	1.69, 1.67

For $\nu = 0.33$, Figure (5b) shows a plot of S^* versus θ for $\nu = 0.33$ and has the same behavior as that of Figure (5a). The crack propagates in the direction of $\theta_o = 0$ at crack velocities of $C = 0.5, 0.6, 0.7$ and 0.8 as predicted by the criterion of the relative minimum strain energy density factor. The crack branching velocity is $0.832 C_2$ and the critical crack angle for branching is 45° . The following table gives the values of strain energy density factors and crack propagation angles with respect to crack velocity.

TABLE 2

SOME CRITICAL VALUES FOR $\nu = 0.33$ IN BROBERG'S MODEL

C/C_2	θ_{cr}	$S_{cr} \cdot \frac{32 \mu}{K_1^2}$
0.5	0°	25.94
0.6	0°	8.13
0.7	0°	2.17
0.8	0°	1.14
0.825	0°	1.03
0.832 (C_{br})	$0^\circ, 45^\circ(\theta_{br})$	1.0056, 1.0080

Similar results are expected for ν equal to other values.

4.2 Yoffé's Model

The Yoffé's model assumes that a crack of fixed length $2a$ is self-sealing and moves at a constant speed C under uniform tension as shown in Figure (3).

For this case, she has found that

$$F_1(S_1, S_2) = [4S_1 S_2 - (1 + S_2^2)]^{-1} \quad (23)$$

Substituting Equation (22) and (23) into (17) for the strain energy density factor, and specifying C/C_2 along with ν , S^* is easily calculated for values of θ from 0° to -90° .

Variations of the strain energy density factor with θ are plotted in Figure (6a), and (6b) for Poisson ratios of 0.25 and 0.33.

The subsequent tables state the theoretical results of θ_{cr} and S_{cr} with $\nu = 0.25$ as well as 0.33.

TABLE 3

SOME CRITICAL VALUES IN YOFFÉ'S MODEL ($\nu = 0.25$)

c/c_2	θ_o	$S_{cr} \cdot \frac{32 \mu}{K_1^2}$
0.5	0°	103.08
0.6	0°	50.73
0.7	0°	31.50
0.8	0°	35.29
0.825 (c_{br})	$0^\circ, 55^\circ (\theta_{br})$	45.60, 45.31

TABLE 4

SOME CRITICAL VALUES IN YOFFÉ'S MODEL ($\nu = 0.33$)

c/c_2	θ_{cr}	$S_{cr} \cdot \frac{32 \mu}{K_1^2}$
0.5	0°	67.80
0.6	0°	31.65
0.7	0°	18.11
0.8	0°	18.30
0.825	0°	22.89
0.832 (c_{br})	$0^\circ, 45^\circ (\theta_{br})$	25.034, 25.095

Figures (7a) and (7b) give plots of S_{cr} versus C/C_2 for the Broberg's and Yoffé's models respectively. Note that the results in Figure (8a) show that branching occurs at a minimum value of S .

Referring to the results of Broberg's and Yoffe's models, crack branching velocity are theoretically the same. This implies that the function $F_1(S_1, S_2)$ does not influence the condition $\partial S / \partial \theta = 0$.

5. DISCUSSION OF RESULTS

It can be concluded from the results in the preceding sections that:

1. Relative minimum of S was found at a crack velocity of $C \simeq 0.5 C_2$ for both the Broberg and Yoffé crack models.
2. In Broberg's model, the strain energy density factor, S , decrease with C/C_2 until branching occurs; while in Yoffé's model S first decreases reaching a minimum at $C/C_2 \simeq 0.75$ and then increases as shown in Figure 7(b).
3. Relatively speaking, crack branching is less likely to occur from material with a higher Poisson's ratio.

In general, it can be said that Yoffé's model is not as realistic as Broberg's. On the other hand Broberg's model is still somewhat away from reality, because of the assumptions of a perfectly sharp crack. In reality, the crack will always attain a finite crack tip radius of curvature. This effect alone will cause large discrepancies between theory and experiment that can not be attributed to the strain energy density factor theory.

Further insights into the crack branching phenomenon may be gained by resolving the strain energy density function into two component parts. One part to represent the energy density due to

change in volume, W_v , and the other part to represent the distortion energy or energy change in shape of the volume element, W_d , i.e.,

$$W = W_v + W_d \quad (24)$$

According to the equations of elasticity,

$$W_v = \frac{1 - 2\nu}{6E} I_1^2 \quad (25)$$

$$W_d = \frac{1 + \nu}{3E} I_1^2 - \frac{1 + \nu}{E} I_2^2 \quad (26)$$

or

$$W_v = \frac{1 - 2\nu}{6E} (\sigma_x + \sigma_y + \sigma_z)^2 \quad (27)$$

$$W_d = \frac{1 + \nu}{3E} (\sigma_x + \sigma_y + \sigma_z)^2 - \frac{1 + \nu}{E} (\sigma_x \sigma_y + \sigma_y \sigma_z + \sigma_z \sigma_x - \sigma_{xy}^2 - \sigma_{yz}^2 - \sigma_{zx}^2) \quad (28)$$

For plane strain, $\sigma_z = \nu (\sigma_x + \sigma_y)$.

Inserting the preceding Equation and Equation (14) into Equation (25), derives Equation (26) in the form

$$W_v = \frac{(1 - 2\nu)(1 + \nu)}{12 \mu} (\sigma_x + \sigma_y)^2 \quad (29)$$

$$W_d = \frac{1}{6\mu} [(1 + \nu)(\sigma_x + \sigma_y)^2] - \frac{1}{2\mu} [\nu(\sigma_x + \sigma_y)^2 + \sigma_x \sigma_y - \sigma_{xy}^2] \quad (30)$$

Equation (26) substituted into terms of S_1 and S_2 by Equation (7), results in

$$W_v = \frac{k_1^2}{r} F_1^2(S_1, S_2) \frac{(1 - 2\nu)(1 + \nu)}{24\mu} \{(1 + S_2^2)(2S_1^2 - S_2^2)\}^2 f^2(S_1) \quad (31)$$

$$\begin{aligned} W_d = & \frac{k_1^2}{r} F_1^2(S_1, S_2) \left(\frac{1 - \nu + \nu^2}{12\mu} \right) \\ & \{(1 + S_2^2)(2S_1^2 - S_2^2)\} f^2(S_1) \\ & + \frac{k_1^2}{r} F_1^2(S_1, S_2) \frac{1}{4\mu} \{(1 + S_2^2)(2S_1^2 + 1 - S_2^2)\} f^2(S_1) \\ & + \frac{k_1^2}{r} F_1^2(S_1, S_2) \frac{4}{\mu} \{S_1^2 S_2^2\} f^2(S_2) \\ & - \frac{k_1^2}{r} F_1^2(S_1, S_2) \frac{1}{\mu} \{S_1 S_2 (1 + S_2^2)(2S_1^2 + 2 \\ & \quad - S_2^2)\} f(S_1) f(S_2) \\ & + \frac{k_1^2}{r} F_1^2(S_1, S_2) \frac{1}{\mu} \{(1 + S_2^2)^2\} g^2(S_1) \\ & + \frac{k_1^2}{r} F_1^2(S_1, S_2) \frac{1}{\mu} \{(1 + S_2^2)^2\} g^2(S_2) \\ & - \frac{k_1^2}{r} F_1^2(S_1, S_2) \frac{2}{\mu} \{(1 + S_2^2)^2\} g(S_1) g(S_2) \end{aligned}$$

S_v and S_d are the strain energy density factors for W_v and W_d respectively, then

$$W_v = \frac{S_v}{r} \quad (33)$$

$$W_d = \frac{S_d}{r} \quad (34)$$

Therefore, strain energy density factor for change in volume is

$$S_v = K_1^2 F_1^2 (S_1, S_2) \frac{(1 - 2\nu)(1 + \nu)}{24\mu} \{(1 + S_2^2)(2S_1^2 - S_2^2)\}^2 f^2(S_1) \quad (35)$$

The distortion energy density factor written as follows:

$$\begin{aligned} S_d = & K_1^2 F_1^2 (S_1, S_2) \left(\frac{1 - \nu + \nu^2}{12\mu} \right) \{(1 + S_2^2)(2S_1^2 - S_2^2)\} f^2(S_1) \\ & + K_1^2 F_1^2 (S_1, S_2) \left(\frac{1}{4\mu} \right) \{(1 + S_2^2)(2S_1^2 + 1 - S_2^2)\} f^2(S_1) \\ & + K_1^2 F_1^2 (S_1, S_2) \left(\frac{4}{\mu} \right) \{S_1^2 S_2^2\} f^2(S_2) \\ & - K_1^2 F_1^2 (S_1, S_2) \left(\frac{1}{\mu} \right) \{S_1 S_2 (1 + S_2^2)(2S_1^2 + 2 - S_2^2)\} f(S_1) f(S_2) \\ & + K_1^2 F_1^2 (S_1, S_2) \left(\frac{1}{\mu} \right) \{(1 + S_2^2)^2\} g^2(S_1) \\ & + K_1^2 F_1^2 (S_1, S_2) \left(\frac{1}{\mu} \right) \{(1 + S_2^2)^2\} g^2(S_2) \end{aligned} \quad (36)$$

$$- K_1^2 F_1^2(S_1, S_2) \left(\frac{2}{\mu}\right) \{(1 + S_2^2)^2\} g(S_1) g(S_2)$$

Equation (35) and (36) can be calculated numerically for different values of C/C_2 and θ on the computer for both the Broberg and Yoffé models.

The numerical solutions of S_v and S_d for crack branching can be summarized into three parts:

- (1) When the crack velocity is approximately less than the distortion-energy density, S_d is larger than the dilatation energy density S_v , i.e., $S_d > S_v$.
- (2) There exists a crack velocity C_p at which both the distortion energy density and dilatation energy density are equal, i.e., $S_d = S_v$.
- (3) When the crack velocity is in the range of $C_p < C < C_b$ where C_b is the crack branching velocity, S_v is always greater than S_d .

The values of $C_p = 0.548 C_2$ and $C_b = 0.825 C_2$ correspond to $v = 0.25$, while $C_p = 0.572 C_2$ and $C_b = 0.832 C_2$ to $v = 0.33$. Note that these values are the same for both the Broberg and Yoffé models.

From equation (7), it is found that $\sigma_{xy} = 0$ along the axis of symmetry $\theta = 0$ which is perpendicular to the tensile load. Therefore, σ_x and σ_y are principal stresses that act on an element ahead of the crack tip.

The ratio of σ_y/σ_x varies as a function of C/C_2 and the numerical results are given in Table 5.

TABLE 5
RATIOS OF σ_y/σ_x FOR BOTH BROBERG'S AND YOFFÉ'S MODEL

ν	C/C_2	0.01	0.05	0.1	0.2	0.3	0.5	0.7	0.8	0.825	0.832
0.25		14998.88	598.87	148.87	36.36	15.50	4.76	1.69	0.87	0.70	
0.33		13399.18	535.18	133.18	32.66	14.03	4.41	1.64	0.88	0.72	0.68

Figure 8(a), 8(b), 9(a) and 9(b) plot S_v , S_d against σ_y/σ_x for a variation of C/C_2 .

For low crack speed, the stress component σ_y is much higher than σ_x as can be seen from Table 5. The material element ahead of the crack is thus subjected to distortion. In fact, the energy density of distortion, S_d , is greater than that of dilatation, S_v .

As the crack velocity C increases the principal stresses σ_x and σ_y are closely equal in magnitude and the difference between S_v and S_d becomes smaller.

At $C = 0.548 C_2$ for $\nu = 0.25$ and $C = 0.572 C_2$ for $\nu = 0.33$ S_v is equal to S_d and the ratio σ_y/σ_x is between 3 and 4. When the crack reaches the critical velocity C_b , S_{\min} occurs at the angles $\pm\theta_b$ measured from both sides of the line of crack extension and $S_v > S_d$.

This phenomenon is obviously due to the additional kinetic energy which cannot be converted fast enough in a single running crack and hence branching occurs.

6. CONCLUSIONS AND SUGGESTIONS FOR FUTURE WORK

It is the opinion of Congleton and Petch (4) that the crack branching can not occur at a constant velocity. The models of Broberg and Yoffé used in the present analysis seem to suggest that material branching is possible for cracks running at constant speeds.

Yoffé has used the maximum shear criterion and predicted a crack branch angle for branch cracks of approximately 60° , while the strain energy density theory yields a value of 55° for $\nu = 0.25$. Sih's theory gives values of $0.832 C_2$ and $0.825 C_2$ for branching.

Both Broberg and Yoffé predicted that the crack will fork at approximately 0.6 times the shear wave velocity.

The Rayleigh wave speed $.92 C_2$ is obviously the upper limit of crack velocity. However, extreme care must be exercised when comparing the above results with experimental data. Sih (8) has shown that crack tip radius of curvature can greatly influence the failure load even for a stationary crack. It is anticipated that the theoretical predictions in crack branching velocity are too high. In reality, the crack will always attain a finite tip radius even though it may be very small. Such an effect will cause the crack to fork at a much lower velocity. It is possible to include an additional term involving ρ/r in the asymptotic expansion of the crack tip's dynamic stresses, where ρ is the crack tip radius of curvature.

Even though the maximum stress criterion predicts crack branching (9), there remains the question whether the criterion gives a reasonable estimate of the experimentally observed crack branching velocity in view of the foregoing comments on the effect of the crack tip radius of curvature.

The strain energy density factor originally presented by Sih (6) to study the fracture of stationary cracks has been extended to study the phenomenon of crack branching. The minimum value of S yields a condition at which at constant velocity, crack changes direction along which the material elements experience more dilatation than distortion. As mentioned earlier, additional work on including the effect of crack tip radius must be carried out before a realistic comparison between theory and experiment could be made.

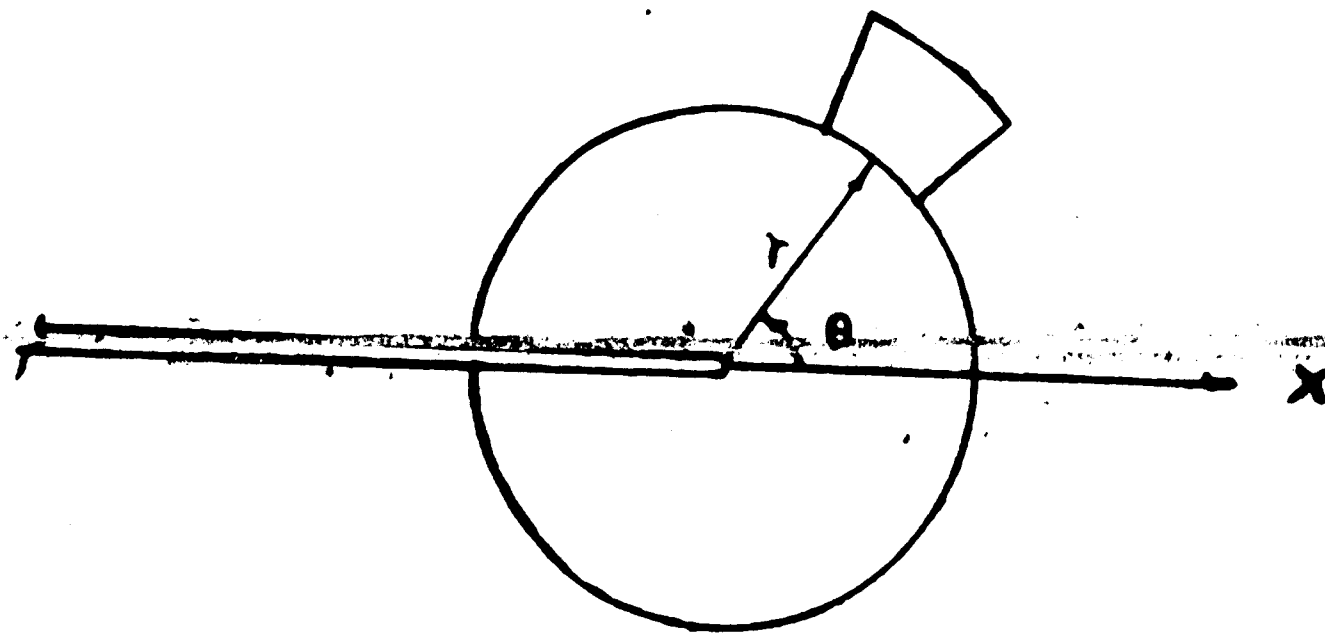


Figure 1 - Coordinates of Element

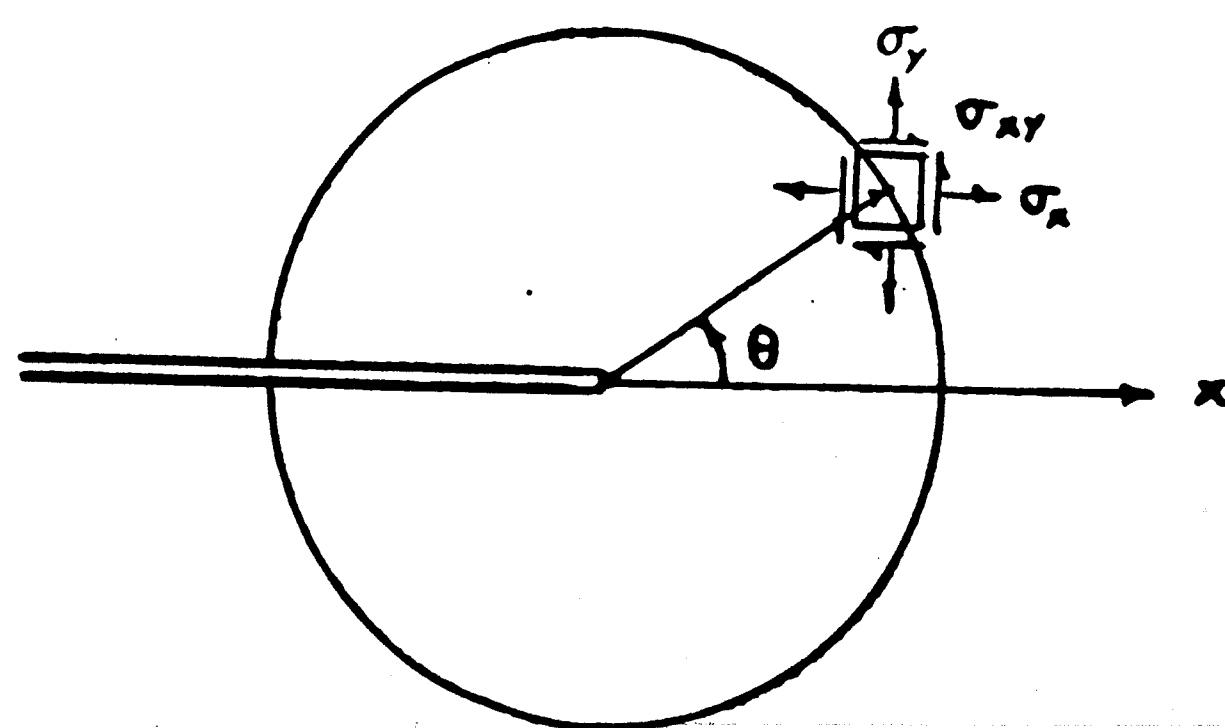


Figure 2 - Stress Element near Crack Tip

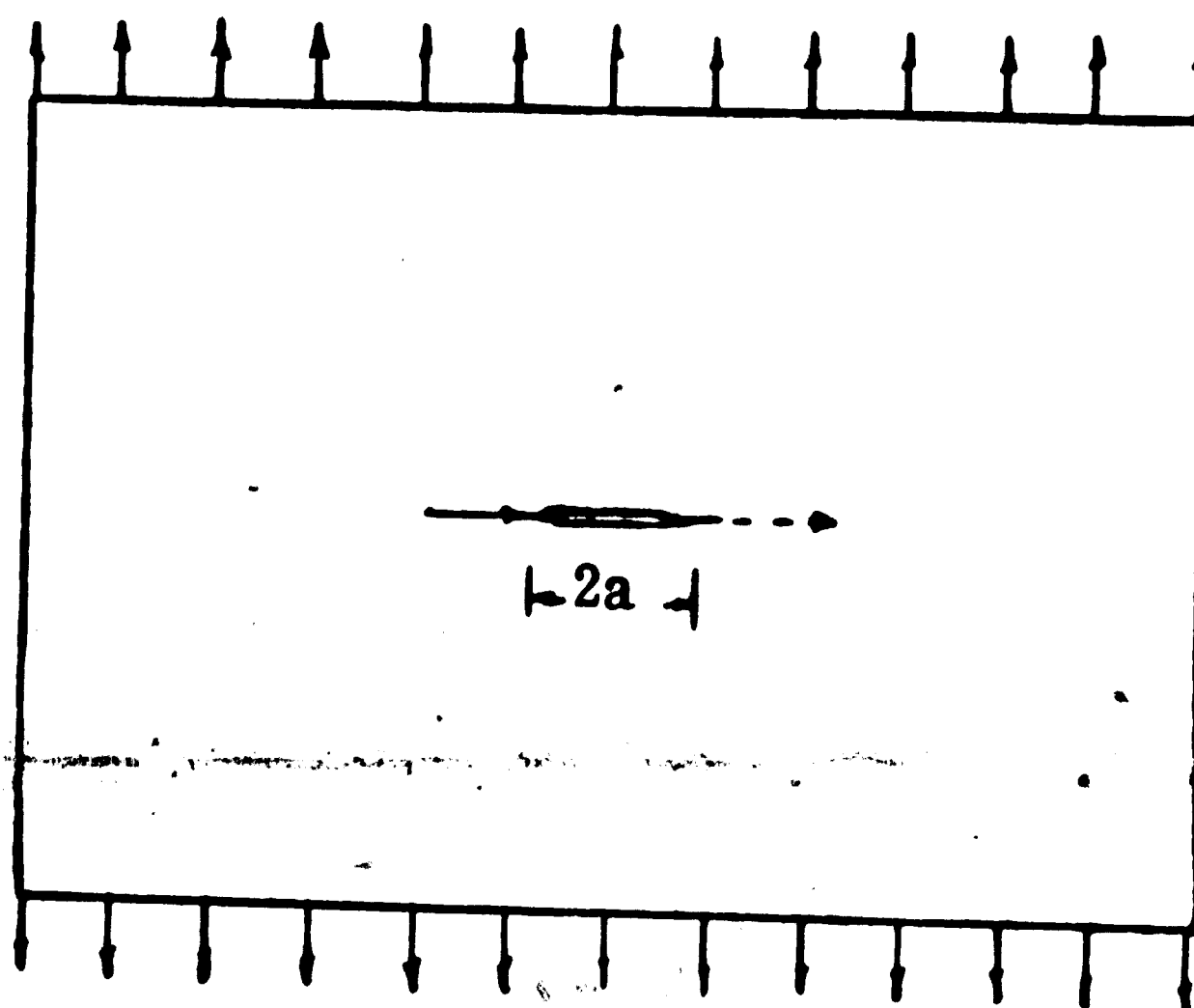


Figure 3 - Crack Configuration of Broberg's Model

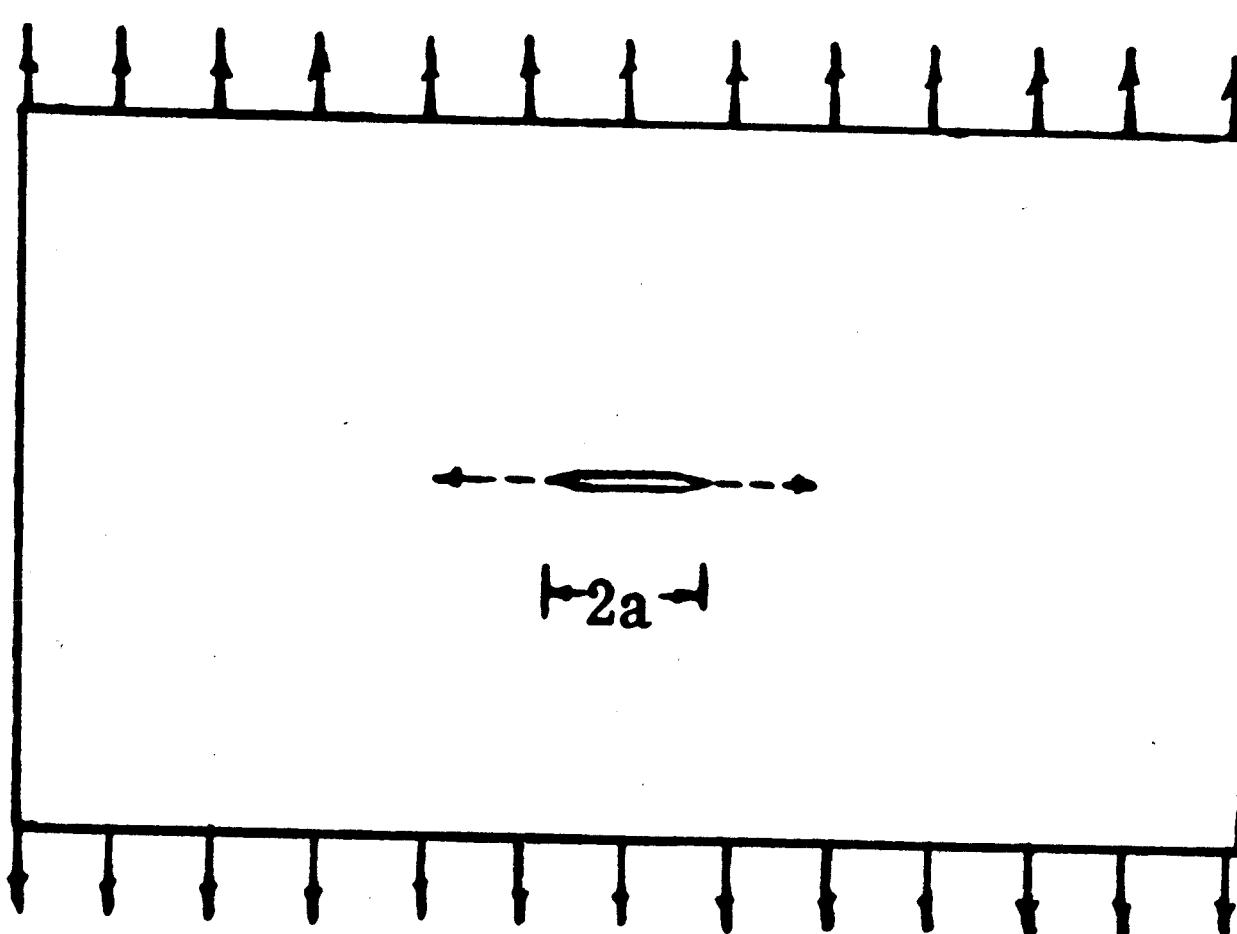


Figure 4 - Crack Configuration of Yoffé's Model

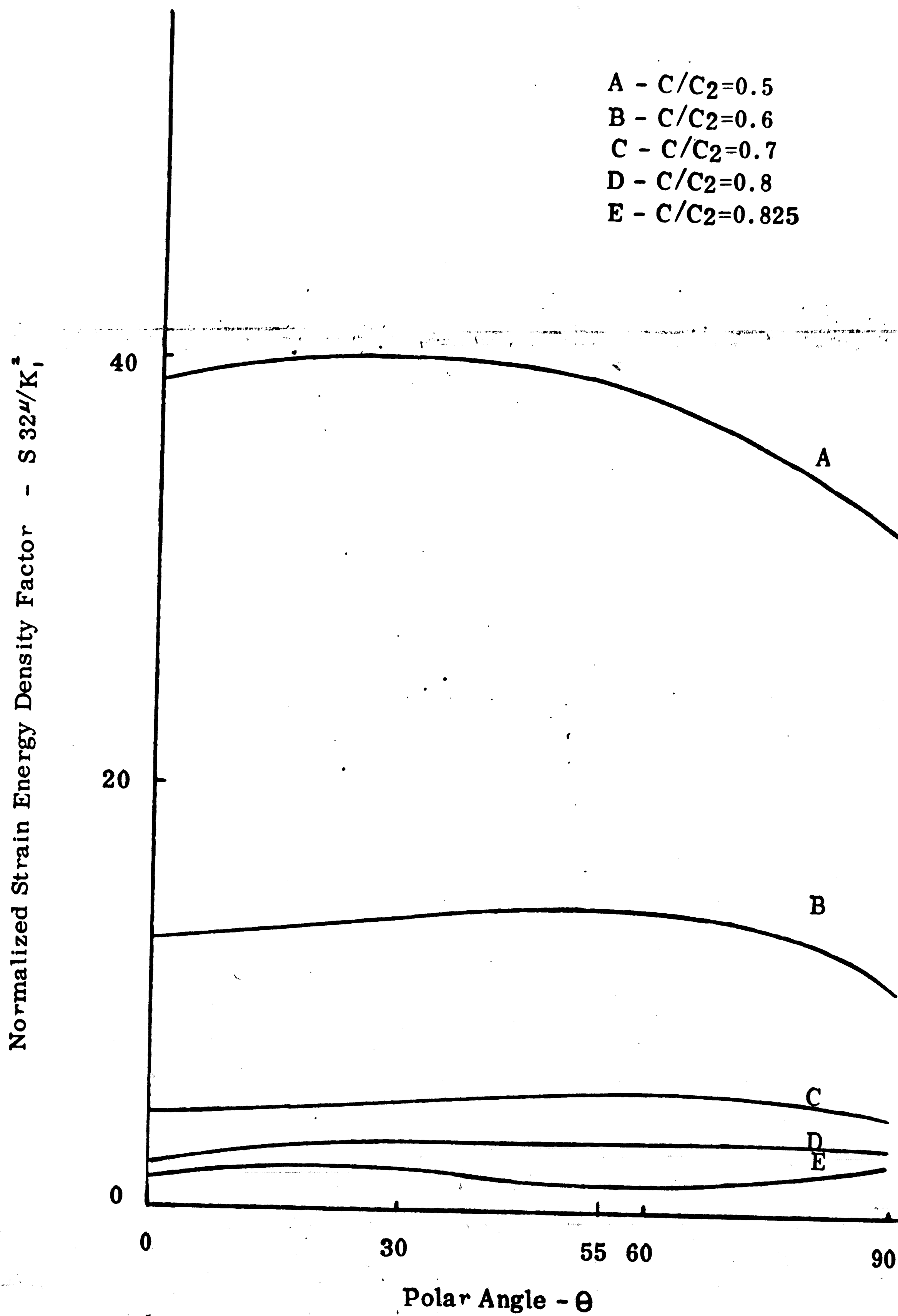


Figure 5(a) - Variation of Strain Energy Density Factor for Broberg's Model ($\nu=0.25$)

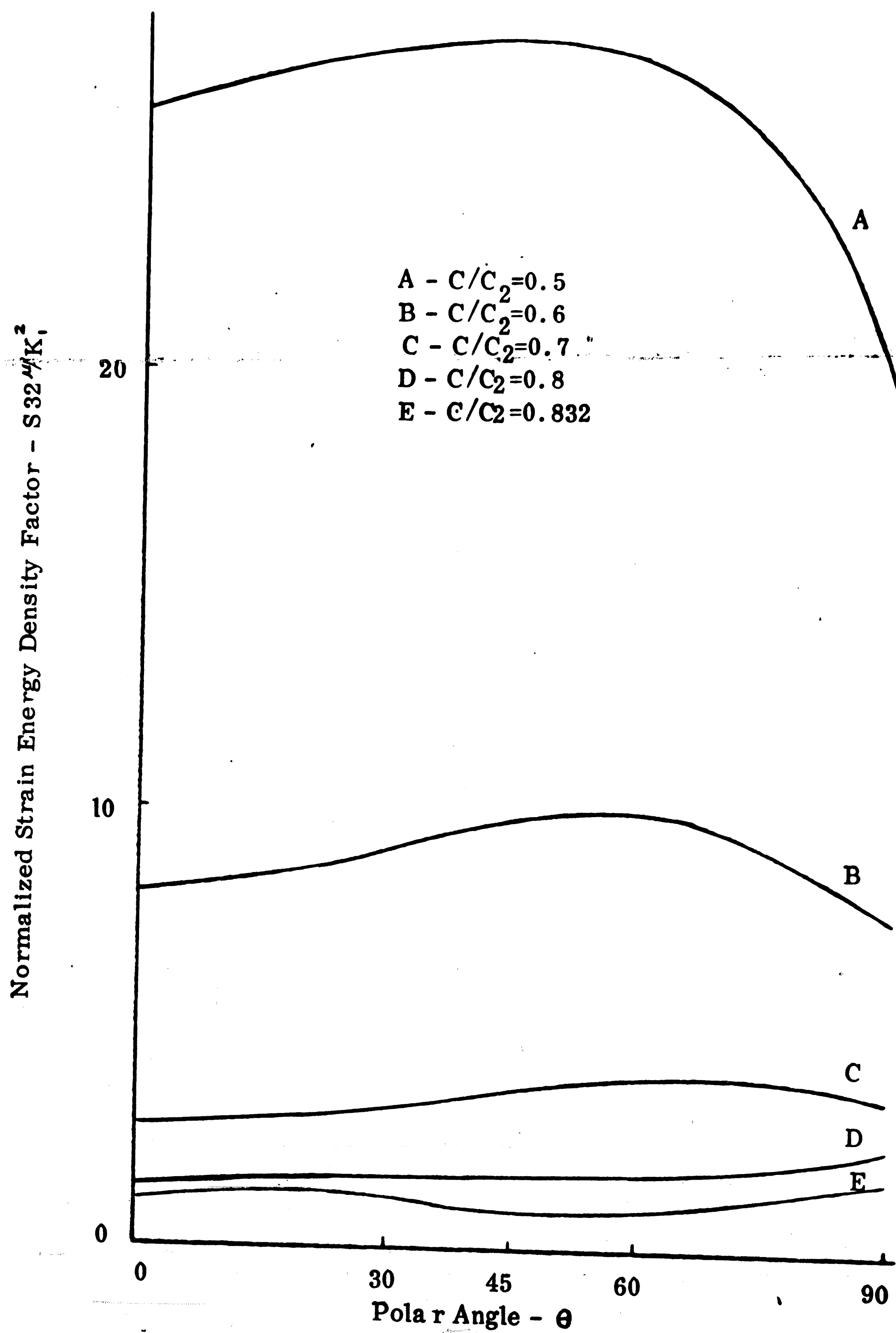


Figure 5(b) - Variation of Strain Energy Density Factor for Broberg's Model ($\nu=0.33$)

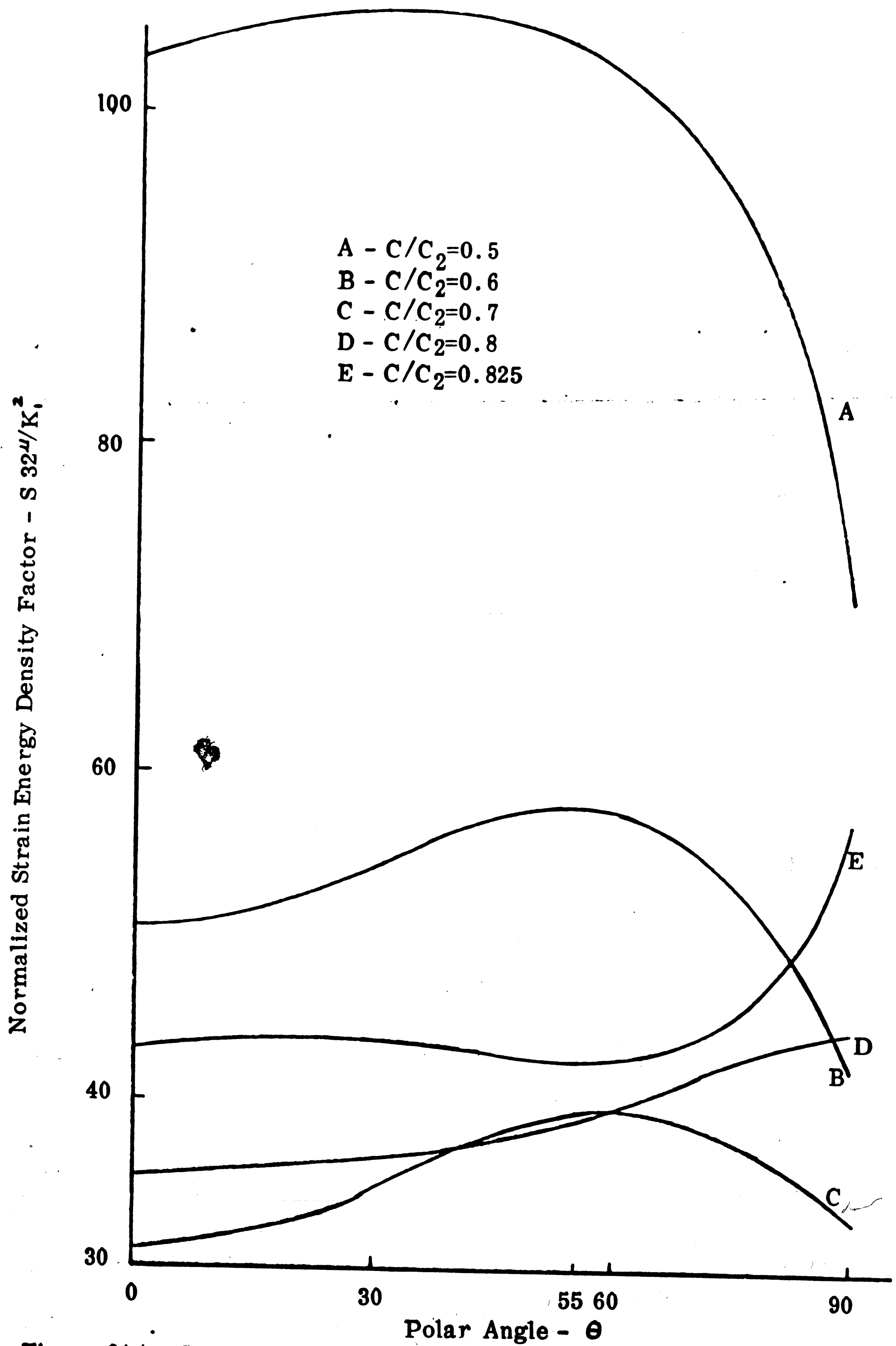


Figure 6(a) - Variation of Strain Energy Density Factor for Yoffé's Model ($\nu=0.25$)

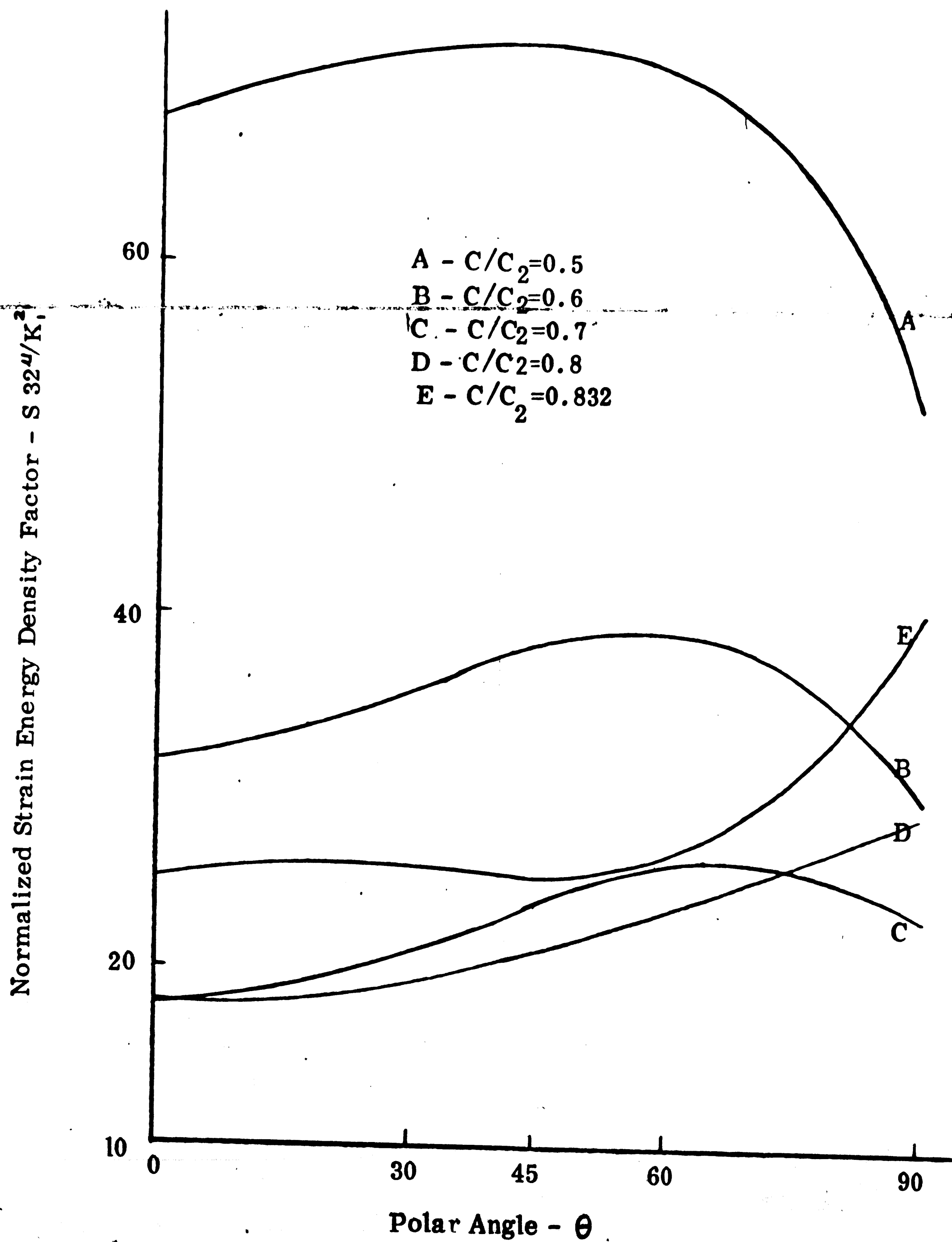


Figure 6(b) - Variation of Strain Energy Density Factor for Yoffé 's Model ($\nu=0.33$)

-33-

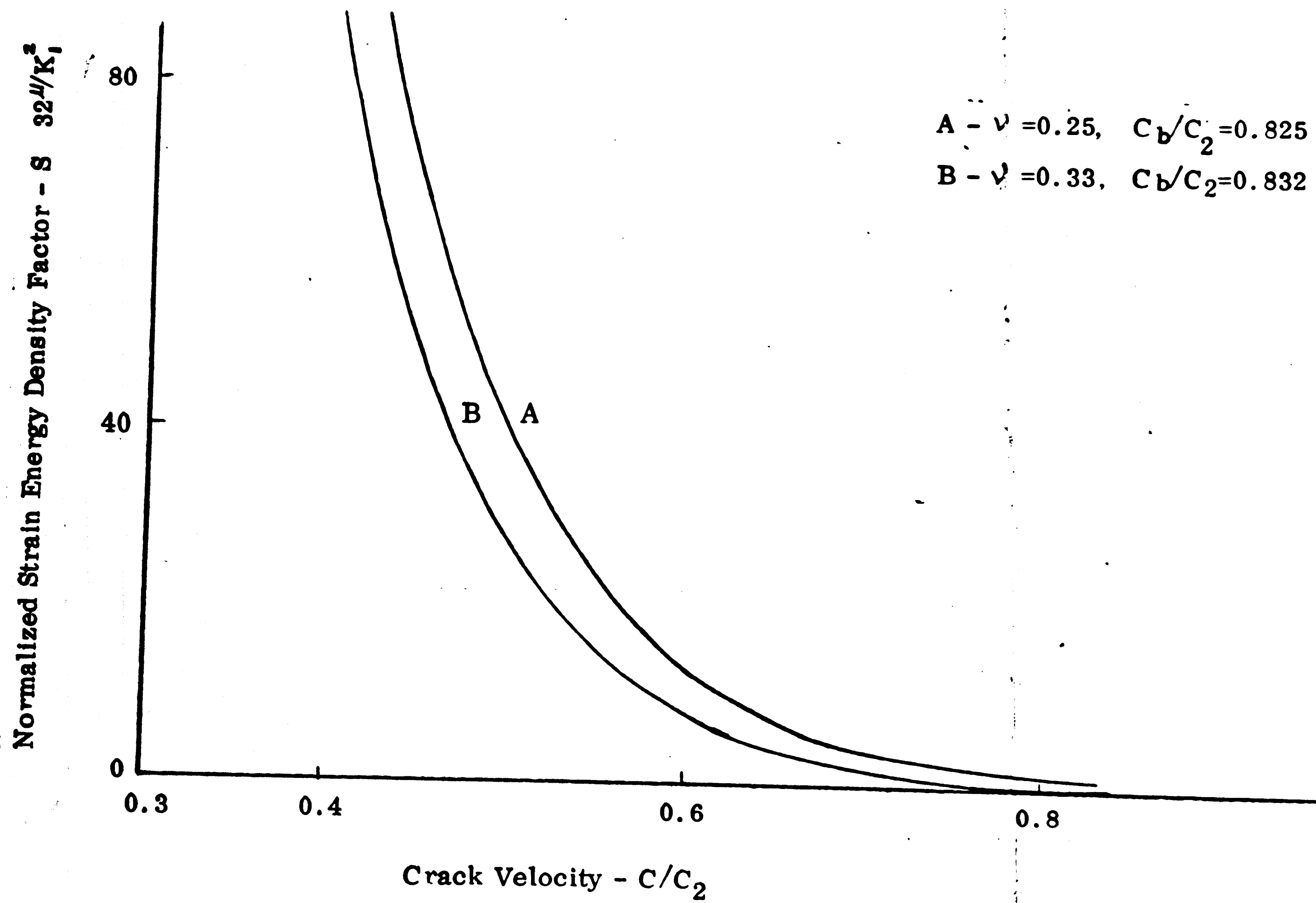


Figure 7(a) - Strain Energy Density Factor versus Crack Velocity (Broberg's Model)

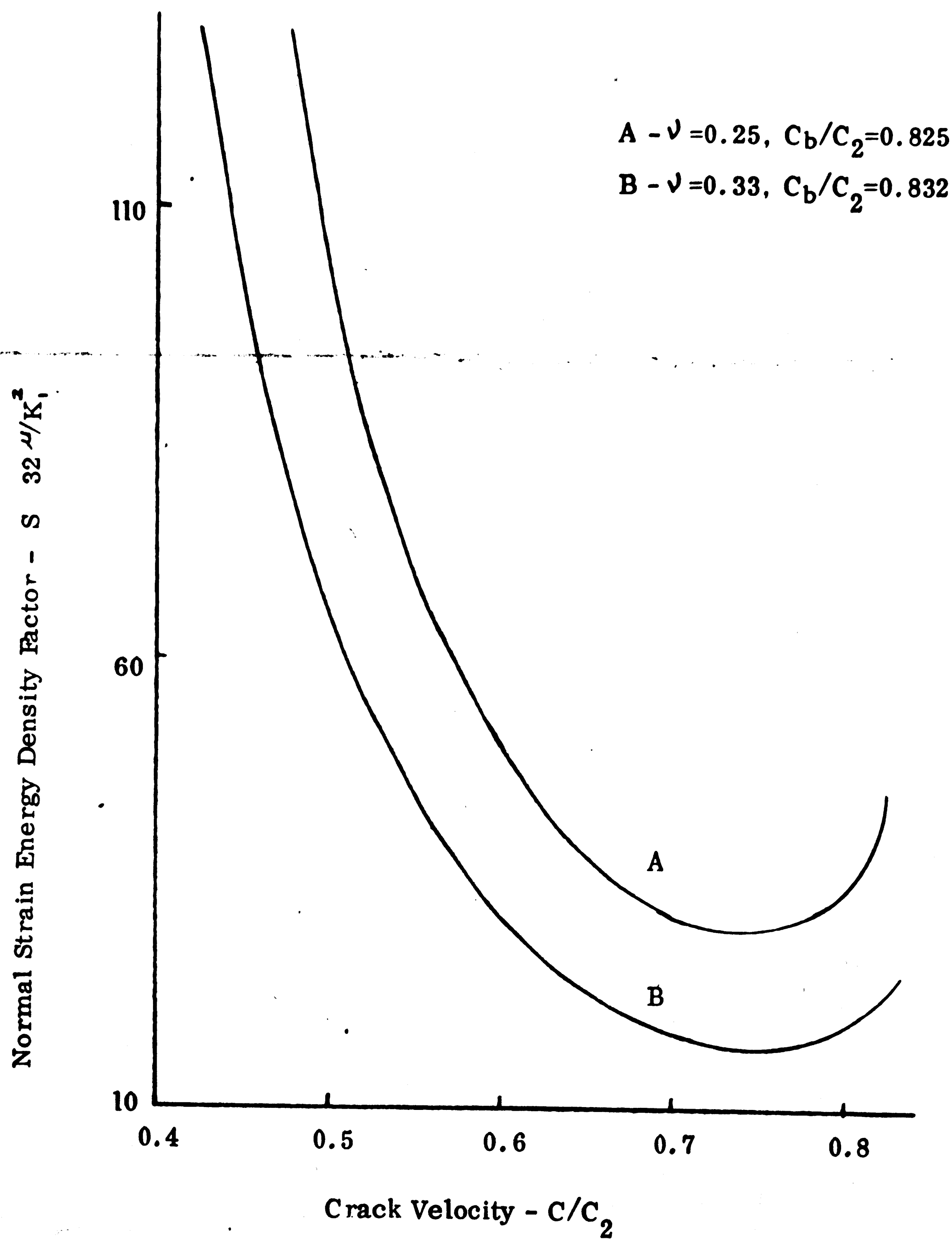


Figure 7(b) - Strain Energy Density Factor versus Crack Velocity
(Yoffé 's Model)

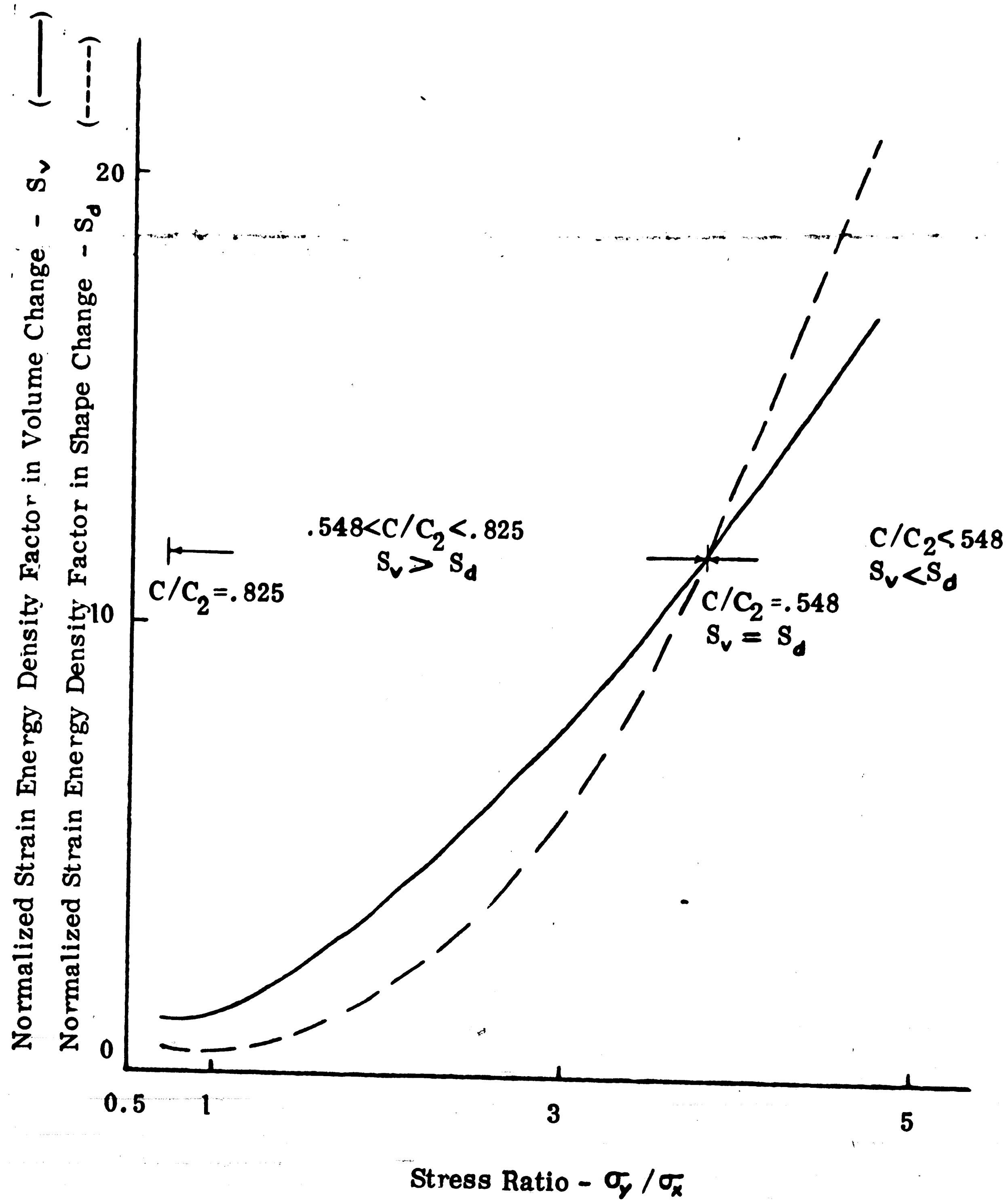


Figure 8(a) Strain Energy Density Factor in Volume Change and Shape Change versus σ_y / σ_x in Broberg's Model ($\nu=0.25$)

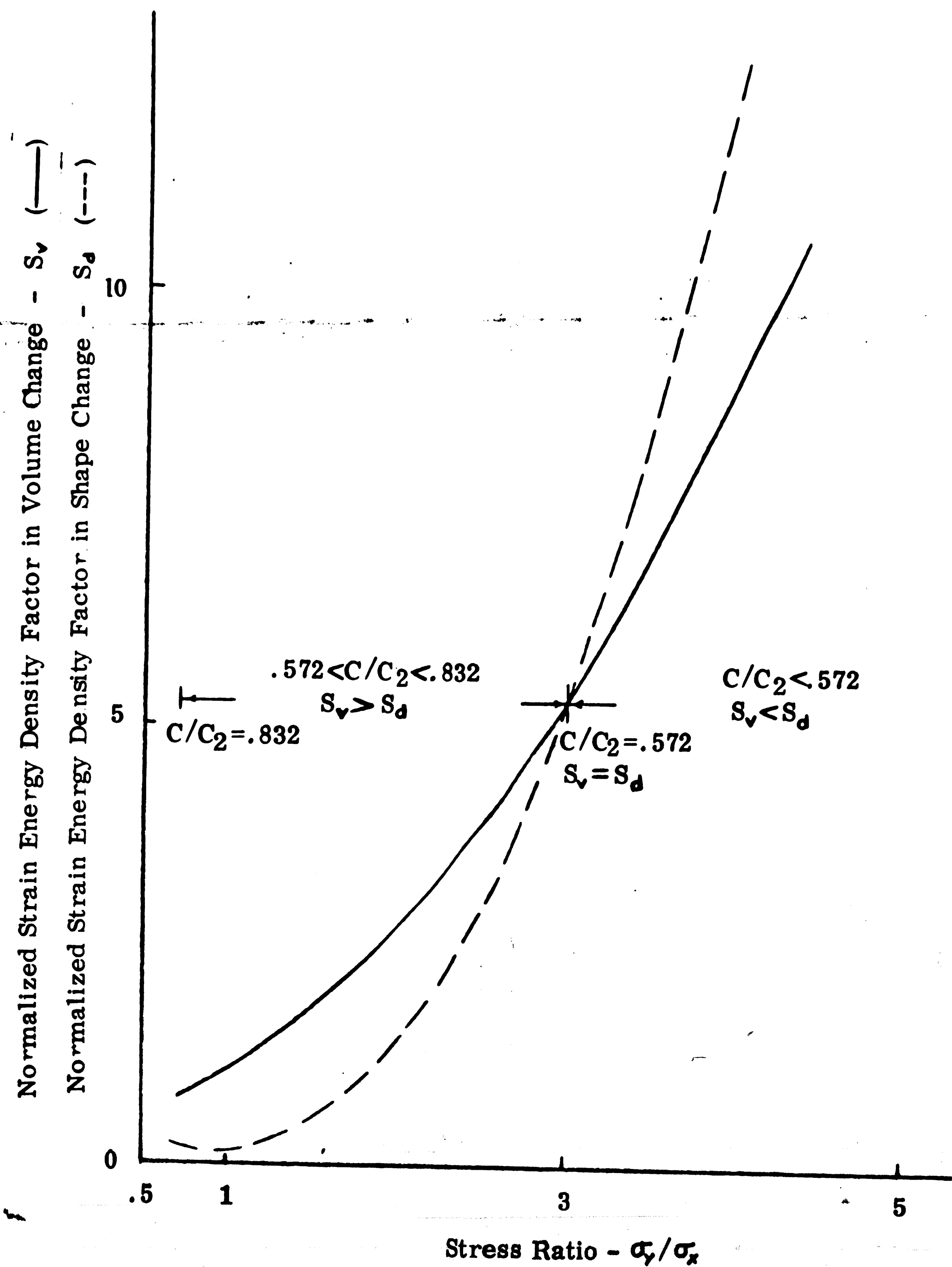


Figure 8(b) - Strain Energy Density Factor in Volume Change and Shape Change versus σ_y/σ_x in Broberg's Model ($\nu=0.33$)

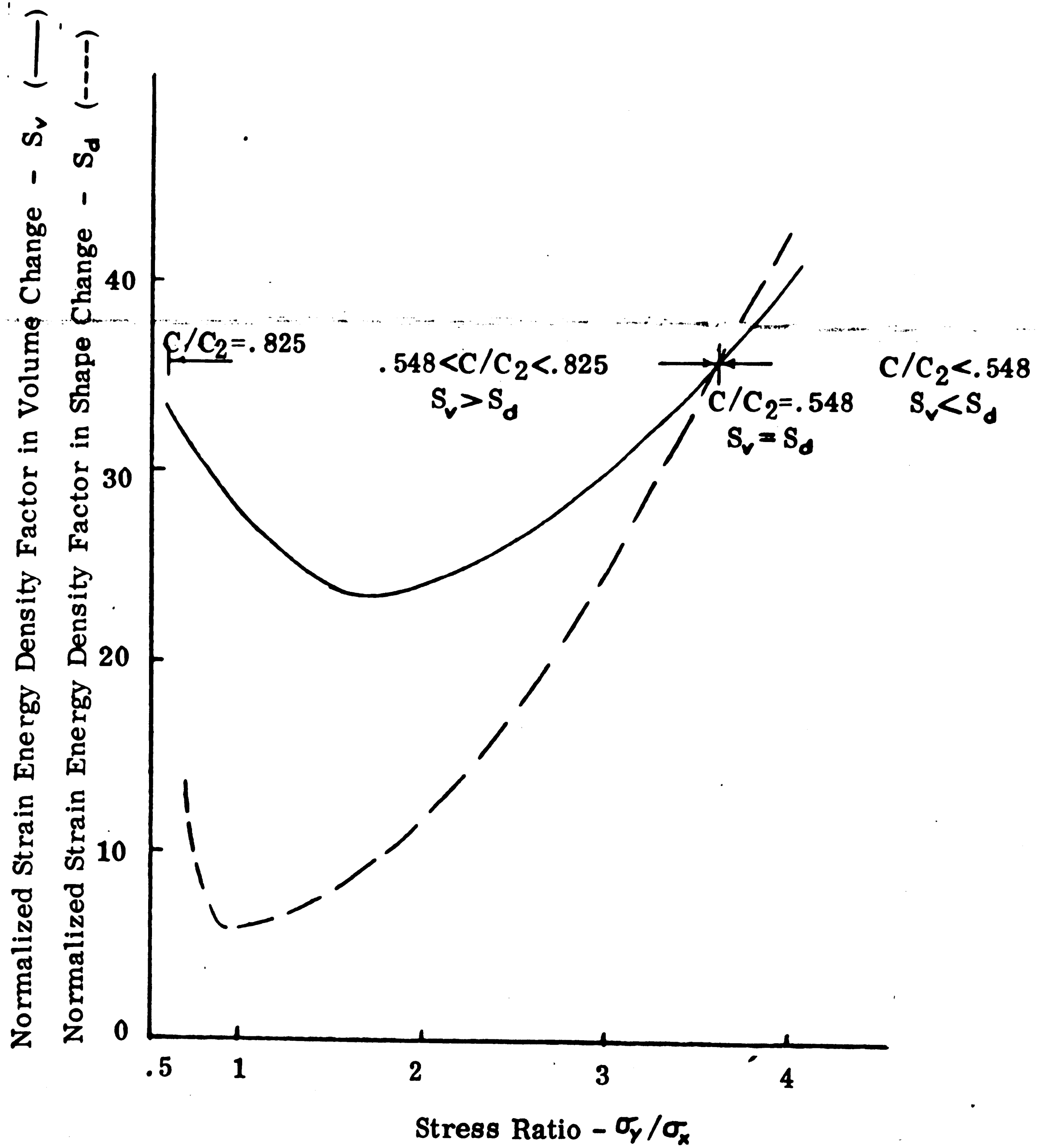


Figure 9(a) - Strain Energy Density Factor in Volume Change and Shape Change versus σ_γ/σ_x in Yoffé's Model ($\nu=0.25$)

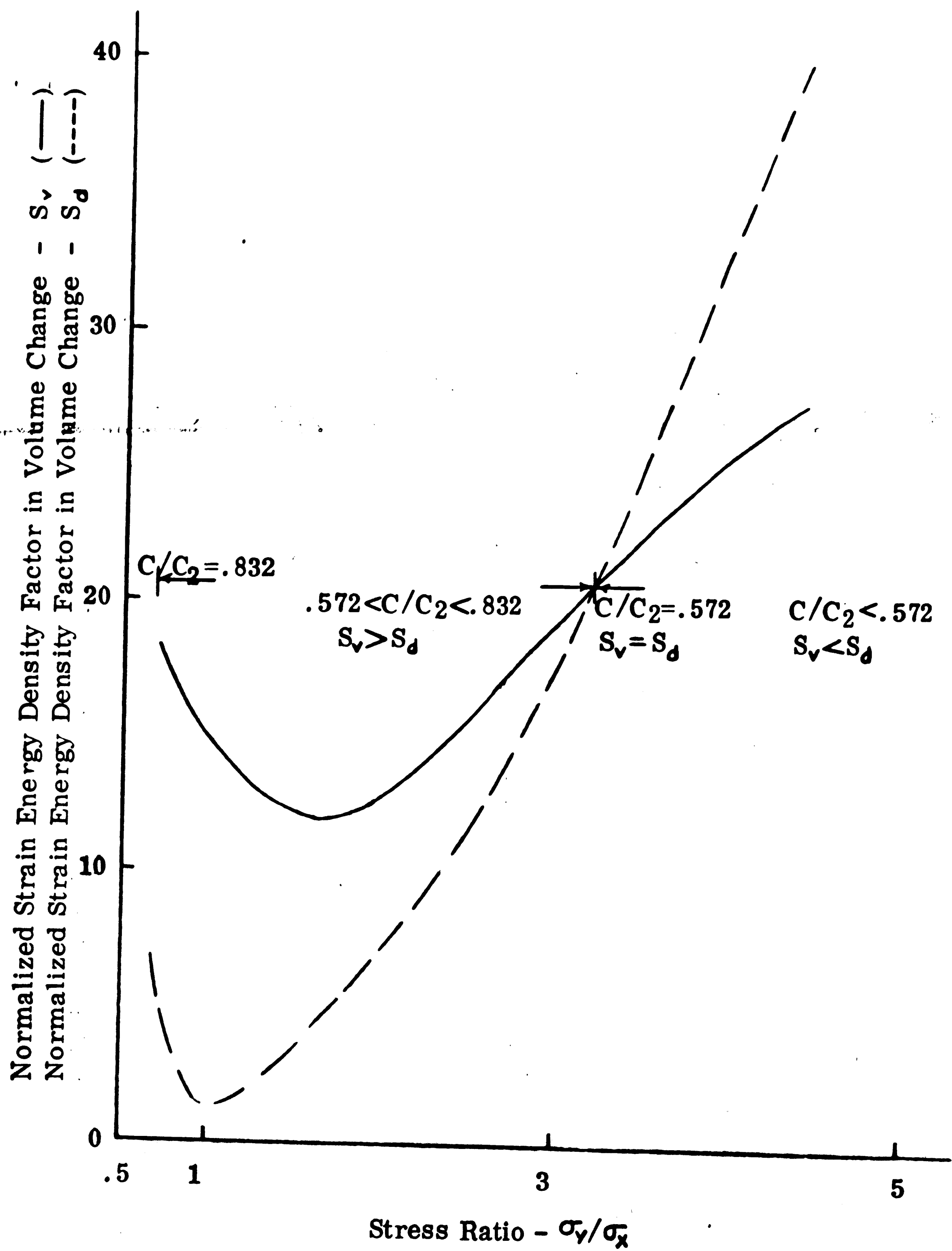


Figure 9(b) - Strain Energy Density Factor in Volume Change and Shape Change versus σ_y/σ_x in Yoffé 's Model ($\nu = 0.33$)

REFERENCES

1. Yoffe, E., 1951, Phil. Mag., 42, 739.
2. Holloway, D. G. and Johnson, J. W., 1966, Phil. Mag., 14, 731
3. Clark, A. B. J. and Irwin, G. R., 1966, Expl. Mech., 23, 321
4. Congleton, J. and Petch, N. J., "Crack Branching", 1967
5. Anthony, S. R., Chubb, J. P. and Congleton, J., "The Crack Branching Velocity", 1970
6. Sih, G. C., "Some Basic Problems in Fracture Mechanics and New Concepts", 1970
7. Sih, G. C., "Dynamics Aspects of Crack Propagation"
8. Sih, G. C., "Application of Strain Energy Density Theory to Fundamental Fracture Mechanics", Proceedings of 10th Anniversary Meeting of Society of Eng. Sci. (in Press)
9. Kerkhof, F., "Wave Fractographic Investigation of Brittle Fracture Mechanics"

VITA

The author was born to Mr. and Mrs. D. C. Han on May 25, 1948 in Chindow, Suntong Provice, China. He attended elementary school and high school in Taipei, Taiwan and graduated in June 1966.

In the fall of that year, he entered the National Taiwan University and received a degree of Bachelor of Science in Civil Engineering.

He began graduate study at Lehigh University in September 1972 under a C. Kemble Baldwin Fellowship and expects to be awarded the degree of Master of Science in Applied Mechanics in May 1974.